Oxygen Evolution

DOI: 10.1002/anie.201306166

Three-Dimensional N-Doped Graphene Hydrogel/NiCo Double Hydroxide Electrocatalysts for Highly Efficient Oxygen Evolution**

*Sheng Chen, Jingjing Duan, Mietek Jaroniec, and Shi Zhang Qiao**

The oxygen evolution reaction (OER), which is a sluggish process, is coupled with a number of key renewable energy systems, such as solar cells, metal–air batteries, and water splitting.[1] Precious metal catalysts such as IrO_2 and RuO_2 show high catalytic activity for the OER,[2] but their applications are limited owing to their high cost and scarcity. As a consequence, various low-cost alternatives have been developed, such as perovskites,[1c] molecular complexes,[3] and first-row transition metal oxides.[4] These materials were generally prepared as two-dimensional (2D) electrocatalysts by dip-coating or drop-casting, which results in low catalyst loadings. Recently, three-dimensional (3D) catalysts were designed by incorporating active species into 3D scaffolds such as nickel foam,[5] which resulted in a significant enhancement of their catalytic activity owing to the higher catalyst loadings and better electrode contact. Note that all the OER catalysts reported to date were prepared in a dehydrated form because water was usually evaporated to enhance immobilization of catalysts on electrodes. Therefore, these catalysts feature relatively poor wettability, limiting their access to electrolytes, and consequently, compromising their activity and kinetics.

Hydrogels are a class of hydrated materials containing large amount of water; thus, they are highly hydrophilic in nature. Among them, graphene hydrogels have received an enormous interest in relation to energy storage and conversion applications because of their unique properties such as high porosity and good network conductivity.[6] Furthermore, these materials possess various functional groups such as carboxyl (−COOH) and hydroxy (−OH),[6] which can interact with water molecules by hydrogen bonding to render them hydrophilic; also, these functional groups can act as anchoring sites to immobilize active nanoparticles. These features make graphene hydrogels attractive scaffolds for designing new hydrated electrocatalysts. However, the major problem associated with graphene is its intrinsically small OER activity, which is usually enhanced by either doping with some heteroatoms or hybridization with transition-metal species. Heteroatoms such as nitrogen (N) are used to alter the charge density of graphene sheets and enhance their catalytic activity.[7] On the other hand, transition-metal species, such as NiCo double oxides/hydroxides, recently gained noticeable popularity in various energy systems owing to their low cost and high theoretical activity.[8] In particular, the Ni and Co species can interact with water molecules to form M−O (M = Ni or Co) bonds and consequently expedite oxygen evolution. To overcome the aforementioned small OER activity of graphene, its hydrogel structure was modified by N-doping and incorporating NiCo species to obtain the N-doped graphene-NiCo double oxide/hydroxide hydrogels that are expected to have high activity and favorable kinetics.

Herein, we report for the first time OER on a 3D-architectured hydrated catalyst, which was fabricated by forming NiCo double hydroxides on N-doped graphene hydrogels. These highly hydrophilic hybrid catalysts (denoted as NG-NiCo) featured favorable electrode kinetics, great durability, and superior activity; the catalytic current of NG-NiCo was much higher than that of the state-of-the-art precious OER electrocatalysts (IrO_2). A significant performance enhancement was achieved owing to the presence of dual active sites originating from the synergy of N-doped graphene and NiCo species. Note that the integration of this catalyst into various devices is easy because of its 3D architecture.

NG-NiCo was prepared in solution as illustrated in Scheme 1. Specifically, graphene oxide (GO) obtained by

Scheme 1. Fabrication of NG-NiCo.

[*] S. Chen, J. J. Duan, Prof. S. Z. Qiao
School of Chemical Engineering, The University of Adelaide
Adelaide, SA 5005 (Australia)
E-mail: s.qiao@adelaide.edu.au
Prof. M. Jaroniec
Department of Chemistry and Biochemistry, Kent State University (USA)

[**] This work is financially supported by the Australian Research Council (ARC) through the Discovery Project programs (DP1095861 and DP130104459).

Supporting information for this article is available on the WWW under http://dx.doi.org/10.1002/anie.201306166.

Hummer's method[9] was converted into a graphene hydrogel by hydrothermal treatment at 150 °C. Then ammonia ($NH_3 \cdot H_2O$) was used to dope graphene sheets with N to obtain an N-doped graphene (NG) hydrogel. In the next step, NiCo double hydroxide was heterogeneously deposited onto NG in a solution containing $Ni(NO_3)_2 \cdot 6H_2O$, $Co(NO_3)_2 \cdot 6H_2O$, and urea to obtain the composite hydrogel material.

The optical image shown in the inset of Figure 1 A reveals that NG-NiCo is a self-supported macroscopic cylinder around 0.8 cm in diameter and several centimeters in length. The black hydrogel is highly hydrophilic, containing 95.3 wt % of water and only 4.7 wt % of the NG-NiCo hybrid catalyst, which exhibits a well-developed 3D interconnected porous network as shown by scanning electron microscopy (SEM, Figure 1 A).

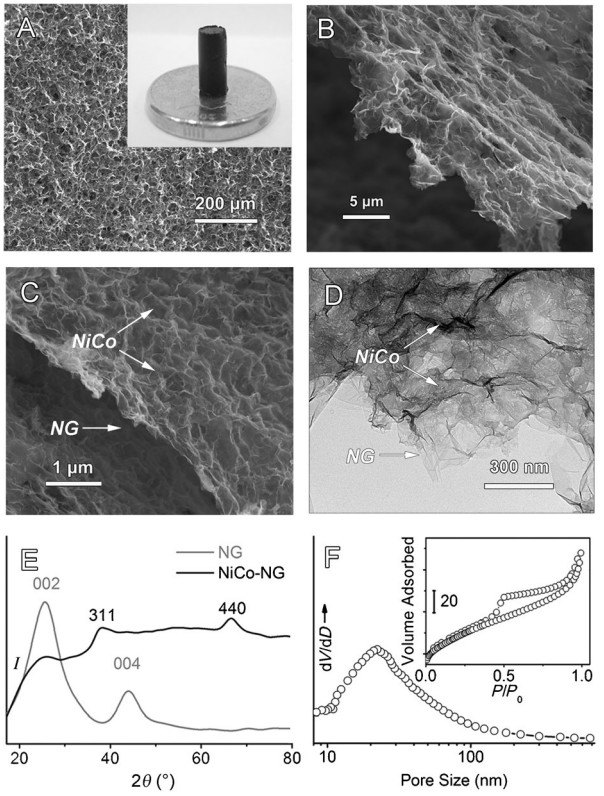

Figure 1. A–C) SEM images of NG-NiCo; the inset in (A) shows an optical image of NG-NiCo. D) A TEM image of NG-NiCo. E) XRD profiles of NG-NiCo and NG. F) The pore size distribution (expressed in $cm^3 g^{-1} nm^{-1}$) of NG-NiCo; the inset in (F) shows the corresponding nitrogen adsorption-desorption isotherm (expressed in cm^3 STP g^{-1}).

Both SEM, low- and high-resolution transmission electron microscopy (TEM), and elemental mappings confirm the deposition of sheet-like NiCo hydroxide species on graphene sheets (Figure 1 B–D; Supporting Information, Figure S1 A–D). In particular, the selected-area electron diffraction (SAED) pattern of NG-NiCo (Supporting Information, Figure S1B) confirms the presence of both graphene (concentric circles) and NiCo species (broad diffuse rings). The evidence of NiCo in hybrid hydrogel is also provided by X-ray diffraction (XRD, Figure 1 E), which reveals two prominent peaks around 37.8° and 66.7° that match well NiCo double hydroxide (JPCDS card no. 20-0781). Further structural characterization of NG-NiCo was obtained with a number of other techniques, including energy-dispersive X-ray spectroscopy (EDS; Supporting Information, Figure S2), Raman spectra (Figure S3A), and thermogravimetric analysis (TGA; Figure S3B), which all confirm the presence of graphene and NiCo components. Moreover, the presence of mesopores in NG-NiCo was verified using nitrogen adsorptions (Figure 1 F), and its high surface area was approved by methlylene blue (MB) experiments (328 $m^2 g^{-1}$; Figure S4 A,B). The mass percentages of NG and NiCo in NG-NiCo are 42.1 and 57.9 w %.

The wettability of NG-NiCo was probed with a Theta/Attension optical tensiometer, which revealed that the hydrogel sample has an average contact angle of 7.3°, in contrast to 54.6° obtained for its dried counterpart (Figure 2 A,B). This result is consistent with Fourier transform

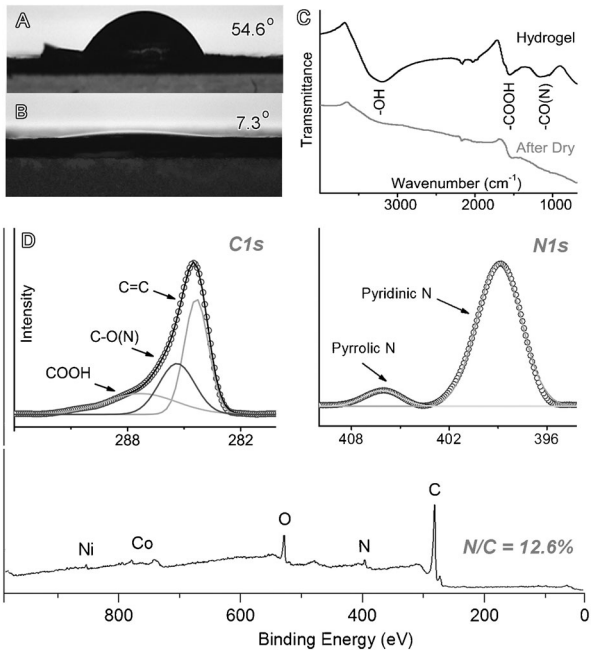

Figure 2. A), B) Contact angle of dried NG-NiCo (A) and NG-NiCo hydrogel (B). C) FTIR spectra of dried and hydrogel NG-NiCo. D) XPS spectra: C1s, N1s, and survey of NG-NiCo.

infrared spectroscopy (FTIR; Figure 2 C) and X-ray photoelectron spectroscopy (XPS; Figure 2 D), which proved the presence of hydrophilic functional groups, such as −COOH, C−OH, or C−NH (denoted as C−O(N)) in NG-NiCo.[7b] Also, XPS revealed the presence of C, O, N, Ni, and Co in NG-NiCo with a N/C ratio of 12.6 %. The N 1s spectrum of NG-NiCo can be deconvoluted into two peaks, that is, pyridinic N (398.8 eV) and pyrrolic N (401.1 eV). The Co 2p spectrum can be fitted by two spin–orbit doublets characteristic of Co^{2+} and Co^{3+} (Figure S4C), and the Ni 2p spectrum by two spin–orbit doublets characteristic of Ni^{3+} (Figure S4D).

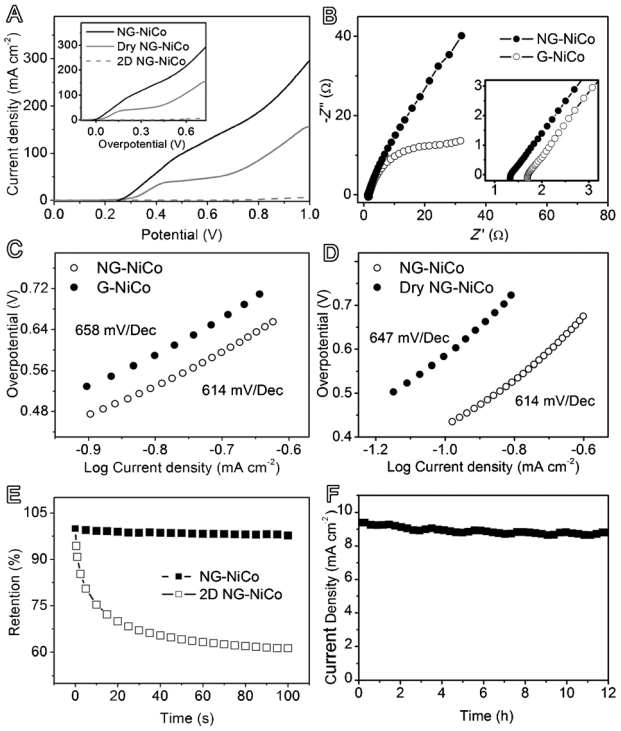

Figure 3. A) LSV plots of NG-NiCo, dried NG-NiCo, and 2D NG-NiCo at 50 mV s^{-1} in 0.1 M KOH; the inset in (A) shows the corresponding data re-plotted as the current density vs. overpotential. B) EIS spectra of NG-NiCo and G-NiCo. C), D) Tafel plots for NG-NiCo in comparison to those for G-NiCo and dried NG-NiCo. E) Retention percentage of the catalytic current for NG-NiCo and 2D NG-NiCo (0.7 V vs. Ag/AgCl) during the initial 100 s. F) Chronoamperometric response for NG-NiCo at 0.5 V vs. Ag/AgCl.

The OER catalytic performance of NG-NiCo was firstly examined by linear scan voltammograms (LSV; Figure 3A; Supporting Information, Figure S5); comparative studies were performed for other samples. Similarly to previous studies,[6b] the working electrodes were prepared by deposition of hydrogels into nickel foams (NF) without any binder or conductive additives (Figure S6, S7). The microstructure of NG-NiCo was not altered in NF (Figure S7), while the contribution of the NF substrate to OER activity was relatively small as compared to NG-NiCo prior the overpotential of 500 mV (Figure S8A). As expected, the NG-NiCo catalyst demonstrated a more negative onset potential of 350 mV than other samples (380 mV for dried NG-NiCo, 447 mV for graphene-NiCo double hydroxide or G-NiCo, 425 mV for two-dimensional N-doped graphene-NiCo double hydroxide or 2D NG-NiCo, 406 mV for NG and 410 mV for NiCo). Moreover, the activities of the aforementioned samples were compared by recording their current densities at the overpotential of 400 mV;[1c] NG-NiCo showed the highest catalytic current density (145.3 mA cm^{-2} vs. 52.6 mA cm^{-2} for dried NG-NiCo, 76.3 mA cm^{-2} for G-NiCo, 2.4 mA cm^{-2} for 2D NG-NiCo, 36.2 mA cm^{-2} for NG and 40.7 mA cm^{-2} for NiCo). Significantly, the current density of NG-NiCo is much higher than that of precious OER catalysts (IrO_2; Figure S8B).[1c] Low overpotential and high catalytic current indicate that NG-NiCo is a highly active OER catalyst.

To gain insight about the effect of N-doping on the OER process, the electrical impedance spectrum (EIS; Figure 3B) was recorded, which revealed NG-NiCo has lower internal resistance (1.3 vs. 1.8 Ohm for G-NiCo) and favorable transport (as indicated by more precipitous slope at a low frequency) as compared to G-NiCo. Also, the Tafel slope of NG-NiCo is smaller than that of G-NiCo (614 vs. 658 mV/Dec, Figure 3C). The lower resistance and smaller Tafel slope correspond to a more favorable OER kinetics over NG-NiCo. On the other hand, the Tafel slope of NG-NiCo obviously increased after freeze-drying (614 vs. 647 mV/Dec for dry NG-NiCo; Figure 3D), indicating the water molecules have a positive effect on the performance of NG-NiCo.

Furthermore, high stability towards OER is critical for electrocatalysts in future energy systems. A 12 h chronoamperometric test of NG-NiCo showed insignificant performance attenuation (< 15%; Figure 3E,F), in contrast to a sharp activity loss of 2D NG-NiCo (> 40% within the first 100 s; Figure 3E). The strong stability of NG-NiCo was also confirmed by LSV (Figure S9A) and Tafel plot (Figure S9B), where only slight alternations were observed after 12 h. Further stability test with the cyclic voltammetry (CV; Figure S10) showed insignificant change in the current densities (at 1 V vs. Ag/AgCl) after 1000 cycles.

The strong durability and enhanced performance indicate that NG-NiCo is an efficient OER catalyst. NiCo oxides/hydroxides have been widely used in various energy systems including OER;[8] however, their activity was lower than that of IrO_2. This study shows that the incorporation of NiCo into an N-doped graphene hydrogel can enhance catalytic activity. Normally, there are three intermediate steps in OER, that is, adsorption of water onto electrode surface, splitting water into molecular oxygen and oxygen evolution. In relation to the first step, NG-NiCo possesses numerous functional groups able to absorb a large amount of water molecules (Figure 2A–C). As regards the second step, NG-NiCo has a highly expanded electrode/electrolyte interface as compared to its dried counterpart (Figure 1F; Supporting Information, Figure S4), which could provide more active sites. Meanwhile, its highly expanded interface allows for an effective oxygen evolution from the electrode in the third step. Therefore, hydrated electrocatalysts are able to facilitate each step of OER, leading to high activity and favorable kinetics (Figure 3A–D; Supporting Information, Figure S5).

Moreover, the high conductivity and well-defined porosity of NG-NiCo contribute to enhanced activity by assuring effective charge and mass transport within electrodes (Figures 1F, 3B; Supporting Information, Figure S4). Interestingly, this study shows that the catalytic currents of NG-NiCo are much less affected by scan rates, with only an insignificant current change (< 10%, 1 V vs. Ag/AgCl) from 10 to 100 mV s^{-1} (Figure S11), underlining the importance of 3D architecture for efficient transport.

Furthermore, the interaction between N-doped graphene and nanoparticles afforded by direct growth of NiCo on graphene contributes to the enhanced OER activity. Controlled experiments reveal the growth duration of 4 h leads to

the optimal catalytic activity (Figure S12). Owing to the high electro-negativity of O or N species, the metal–O–C or metal–N–C might also be present in the hybrid. Therefore, apart from the NiCo species, metal–O–C or metal–N–C might be the other active sites to boost oxidation of water into molecular oxygen. Thus, a dual-active-site mechanism may be responsible for great performance of NG-NiCo in OER. However, it is noteworthy that the NG alone accounts only for about 28 % activity of NG-NiCo (40.7 vs. 145.3 mA cm^{-2} at the overpotential of 400 mV), thus suggesting NiCo might be the main contributor of active sites in the catalyst.

In conclusion, this work reports the first synthesis of a hydrogel-based OER electrocatalyst. The incorporation of ternary hydroxides into N-doped graphene hydrogels has led to excellent catalytic efficiency, making it a promising candidate for next generation of OER catalysts. A significant enhancement in the performance is associated with multiple advantages of N-doped graphene hydrogel, including a multi-dimensional conductive network, rich macro/mesoporosity, high wettability, and N-doping. The resulting catalyst featured also an excellent durability during long-term cycling. Moreover, the material was prepared through a new strategy combining liquid N-doping and post-synthesis incorporation of NiCo hydroxides, thus it is easily adaptable for large-scale preparation. This simple strategy can be easily adapted to prepare other graphene-based 3D catalysts for versatile applications, such as heterocatalysis, metal–air batteries, and photocatalysis.

Received: July 16, 2013
Revised: September 2, 2013
Published online: November 7, 2013

Keywords: metal oxides · nanostructures · N-doped graphene · oxygen evolution reaction

[1] a) H. B. Gray, *Nat. Chem.* **2009**, *1*, 7; b) M. Armand, J. M. Tarascon, *Nature* **2008**, *451*, 652 – 657; c) J. Suntivich, K. J. May, H. A. Gasteiger, J. B. Goodenough, Y. Shao-Horn, *Science* **2011**, *334*, 1383 – 1385.

[2] a) S. Ardizzone, G. Fregonara, S. Trasatti, *Electrochim. Acta* **1990**, *35*, 263 – 267; b) S. Trasatti, *Electrochim. Acta* **1984**, *29*, 1503 – 1512.

[3] a) Q. Yin, J. M. Tan, C. Besson, Y. V. Geletii, D. G. Musaev, A. E. Kuznetsov, Z. Luo, K. I. Hardcastle, C. L. Hill, *Science* **2010**, *328*, 342 – 345; b) E. Mirzakulova, R. Khatmullin, J. Walpita, T. Corrigan, N. M. Vargas-Barbosa, S. Vyas, S. Oottikkal, S. F. Manzer, C. M. Hadad, K. D. Glusac, *Nat. Chem.* **2012**, *4*, 794 – 801.

[4] a) M. R. Gao, Y. F. Xu, J. Jiang, Y. R. Zheng, S. H. Yu, *J. Am. Chem. Soc.* **2012**, *134*, 2930 – 2933; b) L. Trotochaud, J. K. Ranney, K. N. Williams, S. W. Boettcher, *J. Am. Chem. Soc.* **2012**, *134*, 17253 – 17261; c) M. Gong, Y. Li, H. Wang, Y. Liang, J. Z. Wu, J. Zhou, J. Wang, T. Regier, F. Wei, H. Dai, *J. Am. Chem. Soc.* **2013**, *135*, 8452 – 8455.

[5] a) J. Wang, H. X. Zhong, Y. L. Qin, X. B. Zhang, *Angew. Chem.* **2013**, *125*, 5356 – 5361; *Angew. Chem. Int. Ed.* **2013**, *52*, 5248 – 5253; b) Y. H. Chang, C. T. Lin, T. Y. Chen, C. L. Hsu, Y. H. Lee, W. Zhang, K. H. Wei, L. J. Li, *Adv. Mater.* **2013**, *25*, 756 – 760.

[6] a) Y. Xu, K. Sheng, C. Li, G. Shi, *ACS Nano* **2010**, *4*, 4324 – 4330; b) J. Chen, K. Sheng, P. Luo, C. Li, G. Shi, *Adv. Mater.* **2012**, *24*, 4569 – 4573.

[7] a) Y. Xue, J. Liu, H. Chen, R. Wang, D. Li, J. Qu, L. Dai, *Angew. Chem.* **2012**, *124*, 12290 – 12293; *Angew. Chem. Int. Ed.* **2012**, *51*, 12124 – 12127; b) X. Wang, X. Li, L. Zhang, Y. Yoon, P. K. Weber, H. Wang, J. Guo, H. Dai, *Science* **2009**, *324*, 768 – 771.

[8] a) G. Zhang, X. W. Lou, *Adv. Mater.* **2013**, *25*, 976 – 979; b) Y. Li, P. Hasin, Y. Wu, *Adv. Mater.* **2010**, *22*, 1926 – 1929.

[9] W. S. Hummers, R. E. Offeman, *J. Am. Chem. Soc.* **1958**, *80*, 1339 – 1339.

